



Multi-scale modeling of the thermo-viscoelastic behavior of 3D woven composites

Martin Hirsekorn, Lionel Marcin, Thierry Godon

► To cite this version:

Martin Hirsekorn, Lionel Marcin, Thierry Godon. Multi-scale modeling of the thermo-viscoelastic behavior of 3D woven composites. ECCM 20, Jun 2022, Lausanne, Switzerland. hal-03842336

HAL Id: hal-03842336

<https://hal.science/hal-03842336>

Submitted on 7 Nov 2022

HAL is a multi-disciplinary open access archive for the deposit and dissemination of scientific research documents, whether they are published or not. The documents may come from teaching and research institutions in France or abroad, or from public or private research centers.

L'archive ouverte pluridisciplinaire **HAL**, est destinée au dépôt et à la diffusion de documents scientifiques de niveau recherche, publiés ou non, émanant des établissements d'enseignement et de recherche français ou étrangers, des laboratoires publics ou privés.

MULTI-SCALE MODELING OF THE THERMO-VISCOELASTIC BEHAVIOR OF 3D WOVEN COMPOSITES

Martin Hirsekorn^a, Lionel Marcin^b, Thierry Godon^b

a: DMAS, ONERA – Université Paris-Saclay, 29 avenue de la Division Leclerc, 92322 Châtillon, France – martin.hirsekorn@onera.fr

b: Safran Aircraft Engines, Rond point René Ravaud, 77550 Moissy Cramayel, France

Abstract: *A multi-scale modeling strategy is proposed that takes into account the temperature and cure dependence of the viscoelastic behavior of the constituent materials of a composite material and the effects of stress relaxation on thermal expansion and chemical shrinkage. A homogenization strategy is presented, which, starting from the constituent behaviors, yields the homogenized viscoelastic behavior of the composite with time-dependent expansion coefficients. This time-dependence is a direct consequence of the viscoelastic behavior of the constituents, as their expansion coefficients are supposed to be time-independent. In the simulation of a heating process, the model predicts sign changes in the thermal strain rate due to residual stress relaxation close to the glass transition temperature, which cannot be obtained with classical thermo-elastic homogenization methods.*

Keywords: Viscoelasticity; Thermal expansion; Chemical shrinkage; Homogenization

1. Introduction

Fiber reinforced composites with thermosetting polymer matrices are manufactured at much higher temperatures than typical in-service temperatures. During the curing process, the initially liquid resin polymerizes and forms a solid matrix material that holds the fibrous reinforcement together. At the end of the curing process, the composite part is cooled down to room temperature. As the coefficients of thermal expansion (CTE) of the fibers and the matrix material are not the same, residual stresses emerge within the composite, which may lead to part distortion and influence damage onset and evolution [1]. Furthermore, the resin shrinks during polymerization, which also contributes to the formation of residual stresses [2].

While the most common fiber materials (glass or carbon) are in a good approximation linear elastic and independent of temperature over the range of the cure cycle, the behavior of the polymer matrix is viscoelastic, leading to strain and stress evolutions in time even when temperature and degree of cure are constant [3,4]. This time-dependent component of the matrix behavior depends strongly on both temperature and degree of cure [4,5]. Therefore, in most recent published works on modeling residual stresses in composite materials, viscoelastic constitutive laws are used that take into account stress relaxation, which plays an important role in particular at the beginning of the cooling phase, when the matrix is still close to its glass transition temperature T_g [6-8]. The models are either identified directly from experimental observations of the time-dependent behavior of the composite [3] or obtained by viscoelastic homogenization starting from the constituent behaviors [8-11].

To predict residual stresses and shape distortions, time-independent average CTE and coefficients of chemical shrinkage (CCS) are used for the composite [8,11]. This means that

locally, changes of temperature or degree of cure only cause an instantaneous deformation of the material, which does not further evolve in time when temperature and degree of cure are kept constant. However, when looking at the lower scales, it becomes clear that due to the viscoelastic behavior of the matrix, residual stresses caused by, e.g., a temperature change evolve in time due to relaxation and creep phenomena, even if the temperature is kept constant. This effect leads to an evolution of the average strain of the composite after a change of temperature that has to be taken into account by time-dependent CTE (and likewise by time-dependent CCS for the relaxation of the stresses caused by chemical shrinkage).

In this contribution, we show how these phenomena can be taken into account in a multi-scale model of the thermo-viscoelastic behavior of polymer matrix composites with 3D woven reinforcements. The viscoelastic behavior is described in section 2. In section 3, it is shown how time-dependence can be taken into account in CTE and CCS using similar approaches as for the relaxation modulus of the viscoelastic behavior. A recently developed homogenization technique [12] is briefly outlined in section 4. It yields the homogenized viscoelastic behavior and the time-dependent CTE and CCS of the composite from the constituent behaviors. In section 5, the resulting model is used to predict the temperature dependence of the apparent elastic properties and the CTE of the composite.

2. Viscoelastic behavior

2.1 General formulation

We start from the general integral form of linear viscoelasticity, in which the stress tensor is expressed as the Stieltjes convolution of a 4th order tensor of (in general) anisotropic relaxation moduli $\underline{\underline{E}}$ with the mechanical strain $\underline{\underline{\varepsilon}}^{ve}$ over a reduced time ξ

$$\underline{\underline{\sigma}}(\xi) = \int_{-\infty}^{\xi} \underline{\underline{E}}(\xi - \xi') : \frac{\partial \underline{\underline{\varepsilon}}^{ve}(\xi')}{\partial \xi'} d\xi' \quad (1)$$

The mechanical strain is obtained by subtracting the strain due to thermal expansion $\underline{\underline{\varepsilon}}^{th}$ and due to chemical shrinkage $\underline{\underline{\varepsilon}}^{ch}$ from the total strain tensor $\underline{\underline{\varepsilon}}$.

$$\underline{\underline{\varepsilon}}^{ve}(\xi) = \underline{\underline{\varepsilon}}(\xi) - \underline{\underline{\varepsilon}}^{th}(\xi) - \underline{\underline{\varepsilon}}^{ch}(\xi) \quad (2)$$

The reduced time ξ accounts for horizontal shifts of the relaxation curves along the logarithmic time scale upon change of temperature and degree of cure if the time-cure-temperature superposition principle applies [13]

$$\xi(t) = \int_{-\infty}^t \frac{1}{a_T(t')} dt', \quad \xi' = \xi(t') \quad (3)$$

where a_T is the shift factor, which, in general, depends on temperature and degree of cure.

If the relaxation moduli can be approximated by a Prony series

$$\underline{\underline{E}}(\xi - \xi') = \underline{\underline{E}}_{\infty} + \sum_{k=1}^N \underline{\underline{E}}_k e^{-\frac{\xi - \xi'}{\tau_k}} \quad (4)$$

with relaxation times τ_k , the integral form resolves to a generalized Maxwell model given by

$$\underline{\underline{\sigma}}(\xi) = (\underline{\underline{E}}_{\infty} + \sum_{k=1}^N \underline{\underline{E}}_k) : \underline{\underline{\varepsilon}}^{ve}(\xi) - \sum_{k=1}^N \underline{\underline{E}}_k : \underline{\underline{\varepsilon}}_k^{ve}(\xi) \quad (5)$$

with tensorial internal variables $\underline{\varepsilon}_k^{ve}$ accounting for the strain history [14]. They evolve following the differential equations

$$\frac{d\underline{\varepsilon}_k^{ve}(\xi)}{d\xi} = \frac{1}{\tau_k} (\underline{\varepsilon}^{ve}(\xi) - \underline{\varepsilon}_k^{ve}(\xi)) \quad (6)$$

2.2 Viscoelastic model of the matrix

The epoxy matrix used in the modeled composite was characterized experimentally by multi-temperature relaxation tests on fully and partially cured specimens [4]. Relaxation master curves were built for different degrees of cure by shifting the relaxation curves observed at different temperatures along the logarithmic time scale. Below the glass transition temperature, the necessary shift factors can well be approximated by an Arrhenius model:

$$a_T(T, c) = \frac{H(c)}{R \cdot \ln 10} \left(\frac{1}{T} - \frac{1}{T_g(c)} \right) \quad (7)$$

Fitting Prony series to the obtained master curves, it was shown that the coefficients plotted against the relaxation times follow closely a continuous function of the form

$$G(\tau) = A \exp \left(- \left(\frac{\log_{10} \tau - \log_{10} \tau_{peak}}{l_{peak}} \right)^2 \right) + \frac{B}{2} \left(1 - \operatorname{erf} \left(\frac{\log_{10} \tau - \log_{10} \tau_{peak}}{l_{peak}} \right) \right) \quad (8)$$

This function reproduces a Gaussian peak of height A , width l_{peak} , and center position τ_{peak} . For short relaxation times, the curve approximates a constant value of B . erf is the Gaussian error function, which makes the function tend towards zero for long relaxation times. Since this function is continuous, we may freely choose the relaxation times, as long as there is at least one relaxation time per decade. The corresponding weights of the Prony series are then given for the k^{th} relaxation time by

$$G_k = \frac{\log_{10} \tau_{k+1} - \log_{10} \tau_{k-1}}{2} G(\tau_k) \quad (9)$$

The parameters A , B , and l_{peak} are similar for the relaxation master curves obtained from partially cured specimens. The positions of the peaks for different degrees of cure superpose well, if the shift factors are defined with respect to the cure dependent glass transition temperature $T_g(c)$, as written in Eq. (7). T_g as a function of cure is given by the DiBenedetto equation [15]

$$T_g(c) = T_{g0} + (T_{g1} - T_{g0}) \frac{\lambda c}{1 - c(1 - \lambda)} \quad (10)$$

where T_{g0} is the glass transition temperature of the uncured and T_{g1} the glass transition temperature of the fully cured resin. The activation energy H in Eq. (7) decreases with increasing degree of cure. A linear function was used in [9] to take into account this effect.

A 3D version of this model developed in [4] was proposed in [9], based on the assumption of isovolumetric viscous effects. Thus, the tensors \underline{E}_k in the time-dependent terms of Eq. (4) take a purely deviatoric form

$$\underline{E}_k = G_k \left(\underline{\mathbb{1}} - \frac{1}{3} \underline{\mathbb{1}} \otimes \underline{\mathbb{1}} \right) \quad (11)$$

with the coefficients G_k given by Eqs. (8) and (9). The (purely elastic) bulk modulus is included into the time-independent term using for \underline{E}_∞ the general form for an isotropic elastic stiffness

$$\underline{E}_\infty = K \frac{1}{3} \underline{\mathbb{1}} \otimes \underline{\mathbb{1}} + G_\infty \left(\underline{\mathbb{1}} - \frac{1}{3} \underline{\mathbb{1}} \otimes \underline{\mathbb{1}} \right) \quad (12)$$

Here, $\underline{\mathbb{1}}$ is the 2nd order identity tensor and $\underline{\mathbb{1}}$ the 4th order identity tensor with minor symmetry. The assumption of isovolumetric viscous effects implies that for long relaxation times at high temperatures the apparent Poisson ratio tends towards 0.5 [16]. The full list of parameters of the 3D model identified using the experimental data in [4] is given in [9].

3. Time-dependent expansion coefficients

Different formulations were proposed to integrate time-dependent effects of thermal expansion into viscoelastic constitutive models [14,17,18]. They use integral forms similar to the viscoelastic formulation given in Eq. (1) to express the time-dependent effects of thermal expansion on stress or strain. We use the formulation of [18] to write the thermal strain as

$$\underline{\varepsilon}^{th}(\xi) = \int_{-\infty}^{\xi} \underline{\alpha}^{th}(\xi - \xi', T(\xi'), c(\xi')) : \frac{\partial T(\xi')}{\partial \xi'} d\xi' \quad (13)$$

with time-dependent CTE $\underline{\alpha}^{th}$. The chemical shrinkage strain is written in an equivalent form

$$\underline{\varepsilon}^{ch}(\xi) = \int_{-\infty}^{\xi} \underline{\alpha}^{ch}(\xi - \xi', T(\xi'), c(\xi')) : \frac{\partial c(\xi')}{\partial \xi'} d\xi' \quad (14)$$

In the following, we will only show the expressions for the thermal strain, but the same formalism can be applied for the chemical shrinkage strain.

In addition to the reduced time-dependence of $\underline{\alpha}^{th}$ that describes the influence of a temperature change at ξ' on a later time $\xi > \xi'$, we also allow for an explicit dependence of the CTE on temperature and cure at the moment of the temperature change. This is represented by the arguments $T(\xi')$ and $c(\xi')$. As in the case of the relaxation moduli, we suppose that the time-dependence of the CTE can be approximated by a Prony series

$$\underline{\alpha}^{th}(\xi - \xi', T(\xi'), c(\xi')) = \underline{\alpha}_\infty^{th}(T(\xi'), c(\xi')) - \sum_{k=1}^N \underline{\alpha}_k^{th}(T(\xi'), c(\xi')) e^{-\frac{\xi - \xi'}{\tau_k}} \quad (15)$$

The evolution of thermal strain in reduced time is then given by [12]

$$\frac{d\underline{\varepsilon}^{th}(\xi)}{d\xi} = \left(\underline{\alpha}_\infty^{th}(T(\xi), c(\xi)) - \sum_{k=1}^N \underline{\alpha}_k^{th}(T(\xi), c(\xi)) \right) \frac{dT(\xi)}{d\xi} - \sum_{k=1}^N \frac{1}{\tau_k} \underline{\varepsilon}_k^{th}(\xi) \quad (16)$$

with tensorial internal variables $\underline{\varepsilon}_k^{th}$ accounting for the history of temperature and the CTE. They evolve following the differential equations

$$\frac{d\underline{\varepsilon}_k^{th}(\xi)}{d\xi} = \underline{\alpha}_k^{th}(T(\xi), c(\xi)) \frac{dT(\xi)}{d\xi} - \frac{1}{\tau_k} \underline{\varepsilon}_k^{th}(\xi) \quad (17)$$

For time-independent CTE, the classical definition

$$\frac{d\underline{\varepsilon}^{th}(\xi)}{d\xi} = \underline{\alpha}_\infty^{th}(T(\xi), c(\xi)) \frac{dT(\xi)}{d\xi} \quad (18)$$

of the CTE is recovered from Eq. (16).

4. Thermo-viscoelastic homogenization

According to the viscoelastic correspondence principle, the Laplace-Carson (LC) transform

$$\hat{f}(p) = p \int_0^\infty f(\xi) e^{-p\xi} d\xi \quad (19)$$

applied to a viscoelastic problem transforms it into an elastic problem in the LC-space [19] as a function of the transform parameter p . Applying Eq. (19) to Eqs. (1), (13), and (14) yields

$$\hat{\underline{\alpha}}(p) = \hat{\underline{E}}(p) : \left(\hat{\underline{\varepsilon}}(p) - \hat{\underline{\alpha}}^{th}(p) \hat{T}(p) - \hat{\underline{\alpha}}^{ch}(p) \hat{c}(p) \right) \quad (20)$$

if the explicit dependence of $\underline{\alpha}^{th}$ and $\underline{\alpha}^{ch}$ on T and c is momentarily ignored. This corresponds to a thermo-elastic problem as a function of the transform parameter p . Classical thermo-elastic homogenization methods can therefore be applied in the LC-space to obtain the LC-transforms of the relaxation modulus, CTE, and CCS of the homogenized material [12]. Applying the LC-transform to the Prony series expression of the relaxation modulus (Eq. 4) yields for a given value p_i of the LC-transform parameter p

$$\hat{\underline{E}}(p_i) = \underline{E}_\infty + \sum_{k=1}^N \mathcal{L}_{ik} \underline{E}_k \quad (21)$$

with

$$\mathcal{L}_{ik} = \frac{p_i}{p_i + \frac{1}{\tau_k}} \quad (22)$$

Likewise, for a given temperature T and a given degree of cure c , we obtain

$$\hat{\underline{\alpha}}^{th}(p_i, T, c) = \underline{\alpha}_\infty^{th}(T, c) - \sum_{k=1}^N \mathcal{L}_{ik} \underline{\alpha}_k^{th}(T, c) \quad (23)$$

We now assume that the relaxation modulus, CTE, and CCS of the homogenized thermo-viscoelastic behavior can also be well fitted by Prony series, whose weights follow continuous functions if plotted against the relaxation times on a logarithmic time scale. In this case, we can choose to represent the homogenized behavior by the same relaxation times as the matrix behavior, distributing the τ_k uniformly on the logarithmic time scale at one relaxation time per decade [9]. Then, the LC-transforms of the homogenized properties can also be written in terms of Eqs. (21) and (23), with the same transform matrix given by Eq. (22).

If this procedure is carried out for $M \geq N$ different p_i , the coefficients \underline{E}_∞ , \underline{E}_k , $\underline{\alpha}_\infty^{th}$, and $\underline{\alpha}_k^{th}$ of the homogenized behavior can be obtained by solving the least-squares problems given by the equation systems in Eqs. (21) and (23) [9,12]. This problem is often ill-conditioned, causing oscillations in the coefficients of the \underline{E}_k if plotted against the relaxation times [9], which may lead to non-positive definite tensors \underline{E}_k . The proper choice of the p_i [9,19] improves the condition of the least squares problem, which reduces the oscillations [9]. If this is not sufficient, Tikhonov regularization can be used [12] to ensure positive definite \underline{E}_k and thus a thermodynamically admissible homogenized behavior.

5. Results

Two scale changes are needed to obtain the homogenized behavior of a 3D woven composite. In a first step, the homogenized behavior of the warp and weft yarns is determined using a hexagonal representative volume element (RVE) [9] and the thermo-viscoelastic behavior of

the matrix and the fibers (taking zero \underline{E}_k , as the fibers are considered as linear elastic). Time-independent CTE and CCS are taken for the matrix and the fibres [12]. In the second step, the homogenized behaviors of the warp and weft yarns and the matrix behavior are used for thermo-elastic homogenizations on a mesoscopic RVE obtained from micro-tomography images of the composite material [9]. The thermo-elastic homogenizations in the LC-space are carried out by Finite Element (FE) calculations. The resulting homogenized behaviors reproduce accurately the average stresses and strains obtained from full-scale thermo-viscoelastic FE simulations on the respective RVEs using the same FE meshes [9,12].

The homogenized behavior of the composite was used to calculate the evolution of the secant moduli under tensile and shear loading as a function of temperature. The results are compared to experimental data in Figure 1. Up to about 120°C, the model only slightly underestimates the experimental observations. This difference may be due to the influence of the fibers on the polymerization of the resin during composite cure, which is not taken into account, as the predictions were made using exclusively the constituent properties identified on pure matrix specimens. Differences become more significant around T_g , at which the matrix characterization was less accurate due to the very soft and fragile specimens. Above T_g , the resin becomes very soft, and direct interactions between the fibers like friction, which are not taken into account in the model, may influence the apparent properties of the composite.

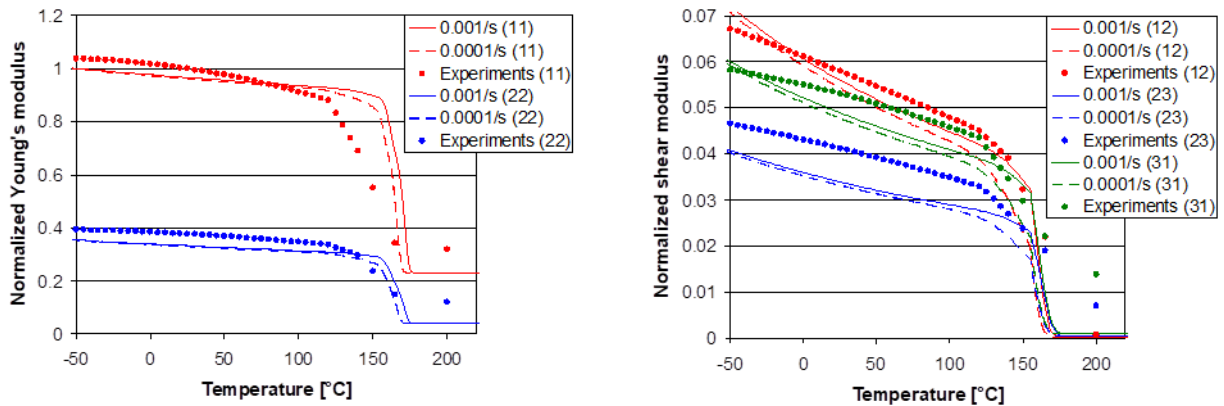


Figure 1. Secant moduli obtained with the homogenized viscoelastic behavior at strain rates of $0.001s^{-1}$ and $0.0001s^{-1}$ compared with experimentally measured moduli of the composite at $0.001s^{-1}$. The moduli are normalized by the measured tensile modulus in warp direction at 25°C.

The evolution of the average composite strain upon heating at 3°C/min from room temperature to 200°C predicted by the homogenized thermo-viscoelastic behavior is shown in Figure 2. The thermal expansion in the out-of-plane direction is significantly larger as in the plane, where it is limited by the fibers. The out-of-plane expansion increases considerably around T_g , as the CTE of the matrix increases. In the plane of the reinforcement, the thermal expansion is initially positive, but gradually slows down at growing temperatures. Close to T_g , the model yields a strong contraction, which is due to the relaxation of the matrix stresses. As a consequence, the composite strain becomes dominated by the fibers, which have a slightly negative CTE. The initially positive strain of the composite disappears when the internal stresses relax, leading to a strongly negative apparent CTE. The model also yields small average shear strains, as the RVE identified from tomography images of the composite, is not perfectly orthotropic with the axes of the coordinate system. These complex evolutions of the average

thermal strain with sign changes of the apparent CTE cannot be predicted by purely thermo-elastic homogenization or by viscoelastic homogenization without taking into account time-dependent effects of the average CTE.

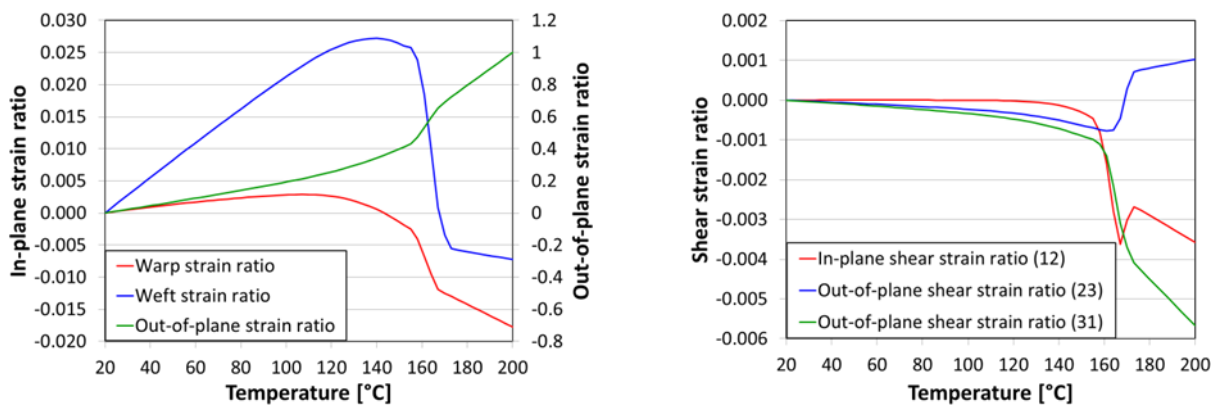


Figure 2. Average strain evolution of the fully cured composite upon heating at 3°C/min predicted by the homogenized thermo-viscoelastic behavior. The strains are normalized by the final out-of-plane strain at 200°C.

6. Conclusions

The viscoelastic behavior of the composite obtained with the presented homogenization method captures well the evolution of the apparent elastic properties with temperature. The time-dependent CTE that take into account stress relaxation at the lower scales predict a sign change of the in-plane average differential CTE of the composite that are not obtained with thermo-elastic or purely viscoelastic homogenization techniques. Experimental validation of the predicted effects is in progress. The presented methodology will be used in multi-scale simulations of the formation of residual stresses and shape distortions of composite parts. In particular, it can give indications on whether the shape of a composite part will evolve in time after the end of the curing process [8] and on relaxation of internal stresses when the parts are reheated.

Acknowledgements

The research presented in this article was funded by the Safran Group, France.

7. References

1. Wisnom MR, Gigliotti M, Ersoy N, Campbell M, Potter KD. Mechanisms generating residual stresses and distorting during manufacture of polymer-matrix composite structures. *Composites: Part A* 2006; 37:522-529.
2. Billotte C, Bernard F, Ruiz E. Chemical shrinkage and thermomechanical characterization of an epoxy resin during cure by a novel in situ measurement method. *European Polymer Journal* 2013; 49:3548-3560.
3. White SR, Kim YK. Process-induced residual stress analysis of AS4/3501-6 composite material. *Mechanics of Composite Materials and Structures* 1998; 5:153-186.

4. Courtois A, Hirsekorn M, Benavente M, Jaillon A, Marcin L, Ruiz E, Lévesque M. Viscoelastic behavior of an epoxy resin during cure below the glass transition temperature: Characterization and modeling. *Journal of Composite Materials* 2018; 53:155-171.
5. O'Brien D, Mather P, White S. Viscoelastic properties of an epoxy resin during cure. *Journal of Composite Materials* 2001; 35:883-904.
6. Zhang J, Zhang M, Li S, Pavier M, Smith D. Residual stresses created during curing of a polymer matrix composite using a viscoelastic model. *Composites Science and Technology* 2016; 130:20-27.
7. Ding A, Li S, Sun J, Wang J, Zu L. A thermo-viscoelastic model of process-induced residual stresses in composite structures with considering thermal dependence. *Composite Structures* 2016; 136:34-43.
8. Benavente M, Marcin L, Courtois A, Lévesque M, Ruiz E. Numerical analysis of viscoelastic process-induced residual distortions during manufacturing and post-curing. *Composites Part A* 2018; 107:205-216.
9. Hirsekorn M, Marcin L, Godon T. Multi-scale modeling of the viscoelastic behavior of 3D woven composites. *Composites Part A* 2018; 112:539-548.
10. Courtois A, Marcin L, Benavente M, Ruiz E, Lévesque M. Numerical multiscale homogenization approach for linearly viscoelastic 3D interlock woven composites. *International Journal of Solids and Structures* 2019; 163:61-74.
11. Trofimov A, Le-Pavic J, Ravey C, Albouy W, Therriault D, Lévesque M. Multi-scale modeling of distortion in the non-flat 3D woven composite part manufactured using resin transfer molding. *Composites Part A* 2021; 140:106145.
12. Hirsekorn M, Marcin L, Godon T. Thermo-viscoelastic homogenization of 3D woven composites with time-dependent expansion coefficients. Submitted to the *International Journal of Solids and Structures* 2022.
13. Eom Y, Boogh L, Michaud V, Sunderland P, Manson J-A. Time-cure-temperature superposition for the prediction of instantaneous viscoelastic properties during cure. *Polymer Engineering and Science* 2000; 40:1281-1292.
14. Sawant S, Muliana A. A thermo-mechanical viscoelastic analysis of orthotropic materials. *Composite Structures* 2008; 83:61-72.
15. Pascault J, Williams J. Relationships between glass transition temperature and conversion. *Polymer Bulletin* 1990; 24:115-121.
16. Tschögl N, Knauss WG, Emri I. Poisson's ratio in linear viscoelasticity – a critical review. *Mechanics of Time-Dependent Materials* 2002; 6(1):3-51.
17. Zocher MA, Groves SE, Allen DH. A three-dimensional finite element formulation for thermoviscoelastic orthotropic media. *International Journal for Numerical Methods in Engineering* 1997; 40:2267-2288.
18. Pettermann H, DeSimone A. An anisotropic linear thermo-viscoelastic constitutive law: Elastic relaxation and thermal expansion creep in the time domain. *Mechanics of Time-Dependent Materials* 2018; 22:421-433.
19. Lévesque M, Gilchrist MD, Bouleau N, Derrien K, Baptiste D. Numerical inversion of the Laplace-Carson transform applied to homogenization of randomly reinforced linear viscoelastic media. *Computational Mechanics* 2007; 40:771-789.